bipolar fashion[25,26]. This suggests that axial and bipolar cues coexist and that the axial cue is normally dominant over the bipolar cue. During mammalian cortical neurogenesis, neural progenitors switch from early symmetric divisions to later asymmetric divisions[27,28]. It will be interesting to determine whether similar mechanisms and molecules are used to control this division symmetry switch in mammals. Together with some recent studies[29], our results on E-APC highlights the importance of tumour suppressors in regulating not only cell growth but also polarity and asymmetric division. □

Methods

Fly stocks and genetics

We used the *UAS-GAL4* system to express ectopically *UAS–Pon–GFP* and *UAS–tau–GFP* (a gift from A. Brand) constructs in epithelial cells under the control of a maternal *V32A–GAL4* driver (a gift from D. St Johnston). For the RNA interference experiment, virgin females from a homozygous recombinant line of *V32A–GAL4* and *UAS–Pon–GFP* were crossed to males from a homozygous *UAS-tau–GFP* line, and embryos were collected for injection. For the overexpression of Crb-intra, we crossed virgin females from a homozygous recombinant line of *V32A–GAL4* and *UAS–Pon–GFP* to males from a homozygous *UAS–Crb-intra* line (a gift from A. Wodarz). For characterization of epithelial cell division in *crumbs* mutant, *V32A-GAL4–UAS-Pon–GFP/+; crb*^{11A22}*/+* virgin females were crossed to males of the same genotype. Embryos produced from the above cross were aged to stages 9–10 and then processed for *in vivo* imaging study[30].

RNAi and *in vivo* imaging

Double-stranded RNAs were produced by *in vitro* transcription using polymerase chain reaction (PCR) products tagged at both ends with T7 RNA polymerase promoter sequences. The following PCR primers were used to generate the templates: dEB1, 5′-GGATCCTAATACGACTCACTATAGGGAGGAGCCAGGAATCATTTAGTTCTCCG; dEB1, 3′-GGATCCTA ATACGACTCACTATAGGGAGGCGCTCCTTTTCCAATCCCT CCAGG; E-APC, 5′-GGATCCTAATACGACTCACTATAGGGAGGGAGTCGGAGGGTG AGCCGCCGGGG; E-APC, 3′-GGATCCTAATACGACTCACTATAGGGAGGTGCTGC AACTTGTAATAATTAAGCAGCTGGC; crb, 5′-GGATCCTAATACGACTCACTATAGGG AGGT GGAAATGGACAACGTACTGAAGCC; crb, 3′-GGATCCTAATACGACTCACTA TAGGGAGGTACTCGCGTATATATAGGCATATAGG; baz, 5′-GGATCCTAATAC GACTC ACTATAGGGAGGCCGCCCAGCAGCAACAGTTGGCAC; baz, 3′-GGATCCTAATAC GACTCACTATAGGGAGGGACGTAGTGTCTCCATGGCCTCGGC. Double-stranded RNAs were injected into Pon–GFP and tau–GFP transgenic embryos as described[17]. Aged embryos were subjected to *in vivo* imaging analysis[30].

Immunohistology

For immunostaining of wild-type and *crb(RNAi)* embryos, we processed an overnight collection of mixed-stage wild-type embryos, or *crb* dsRNA-injected embryos aged to stages 10–12 as described[10]. We used the following primary antibodies: rabbit anti-EAPC (a gift from M. Bienz), mouse anti-Tubulin (Sigma), rat anti-E-cadherin (a gift from T. Uemura), guinea pig anti-Asense, rabbit anti-Insc (a gift from B. Chia) and mouse anti–GFP (Molecular Probes), rat anti-Bazooka (a gift from A. Wodarz). Images were recorded on a confocal microscope and processed with Photoshop.

Received 20 October; accepted 20 November 2000.

1. Lu, B., Jan, L. Y. & Jan, Y. N. Control of cell divisions in the nervous system: symmetry and asymmetry. *Annu. Rev. Neurosci.* **23,** 531–556 (2000).
2. Jan, Y. N. & Jan, L. Y. Polarity in cell division: what frames thy fearful asymmetry? *Cell* **100,** 599–602 (2000).
3. Yu, X., Waltzer, L. & Bienz, M. A new *Drosophila* APC homologue associated with adhesive zones of epithelial cells. *Nature Cell Biol.* **1,** 144–151 (1999).
4. Korinek, W. S., Copeland, M. J., Chaudhuri, A. & Chant, J. Molecular linkage underlying microtubule orientation toward cortical sites in yeast. *Science* **287,** 2257–2259 (2000).
5. Lee, L. *et al.* Positioning of the mitotic spindle by a cortical-microtubule capture mechanism. *Science* **287,** 2260–2262 (2000).
6. Kraut, R. & Campos-Ortega, J. A. *inscuteable*, a neural precursor gene of *Drosophila*, encodes a candidate for a cytoskeleton adapter protein. *Dev. Biol.* **174,** 65–81 (1996).
7. Kraut, R., Chia, W., Jan, L. Y., Jan, Y. N. & Knoblich, J. A. Role of *inscuteable* in orienting asymmetric cell division in *Drosophila*. *Nature* **383,** 50–55 (1996).
8. Ikeshima-Kataoka, H., Skeath, J. B., Nabeshima, Y., Doe, C. Q. & Matsuzaki, F. Miranda directs Prospero to a daughter cell during *Drosophila* asymmetric divisions. *Nature* **390,** 625–629 (1997).
9. Shen, C-P., Jan, L. Y. & Jan, Y. N. Miranda is required for the asymmetric localization of Prospero during mitosis in *Drosophila*. *Cell* **90,** 449–458 (1997).
10. Lu, B., Rothenberg, M., Jan, L. Y. & Jan, Y. N. Partner of Numb colocalizes with Numb during mitosis and directs Numb asymmetric localization in *Drosophila* neural and muscle progenitors. *Cell* **95,** 225–235 (1998).
11. Kuchinke, U., Grawe, F. & Knust, E. Control of spindle orientation in *Drosophila* by the Par-3-related PDZ-domain protein Bazooka. *Curr. Biol.* **8,** 1357–1365 (1998).
12. Wodarz, A., Ramrath, A., Kuchinke, U. & Knust, E. Bazooka provides an apical cue for Inscuteable localization in *Drosophila* neuroblasts. *Nature* **402,** 544–547 (1999).
13. Schober, M., Schaefer, M. & Knoblich, J. A. Bazooka recruits Inscuteable to orient asymmetric cell divisions in *Drosophila* neuroblasts. *Nature* **402,** 548–551 (1999).
14. Yu, F., Morin, X., Cai, Y., Yang, X. & Chia, W. Analysis of Partner of Inscuteable, a novel player of *Drosophila* asymmetric divisions, reveals two distinct steps in Inscuteable apical localization. *Cell* **100,** 399–409 (2000).
15. Schaefer, M., Shevchenko, A., Shevchenko, A. & Knoblich, J. A. A protein complex containing Inscuteable and the Gα-binding protein Pins orients asymmetric cell divisions in *Drosophila*. *Curr. Biol.* **10,** 353–362 (2000).
16. Tepass, U. Epithelial differentiation in *Drosophila*. *BioEssays* **19,** 673–682 (1997).
17. Kennerdell, J. R. & Carthew, R. W. Use of dsRNA-mediated genetic interference to demonstrate that Frizzled and Frizzled 2 act in the Wingless pathway. *Cell* **95,** 1017–1026 (1998).
18. Fire, A. *et al.* Potent and specific genetic interference by double-stranded RNA in *Caenorhabditis elegans*. *Nature* **391,** 806–811 (1998).
19. Wodarz, A., Hinz, U., Engelbert, M. & Knust, E. Expression of *crumbs* confers apical character on plasma membrane domains of ectodermal epithelia. *Cell* **82,** 67–76 (1995).
20. Klebes, A. & Knust, E. A conserved motif in Crumbs is required for E-cadherin localisation and zonula adherens formation in *Drosophila*. *Curr. Biol.* **10,** 76–85 (2000).
21. Muller, H. A. & Wieschaus, E. *armadillo, bazooka*, and *stardust* are critical for early stages in formation of the zonula adherens and maintenance of the polarized blastoderm epithelium in *Drosophila*. *J. Cell Biol.* **134,** 149–163 (1996).
22. McCartney, B. M. *et al.* *Drosophila* APC2 is a cytoskeletally-associated protein that regulates wingless signaling in the embryonic epidermis. *J. Cell Biol.* **146,** 1303–1318 (1999).
23. Su, L. K. *et al.* APC binds to the novel protein EB1. *Cancer Res.* **55,** 2972–2977 (1995).
24. Nathke, I. S., Adams, C. L., Polakis, P., Sellin, J. H. & Nelson, W. J. The adenomatous polyposis coli tumor suppressor protein localizes to plasma membrane sites involved in active cell migration. *J. Cell Biol.* **134,** 165–179 (1996).
25. Chant, J. & Herskowitz, I. Genetic control of bud site selection in yeast by a set of gene products that constitute a morphogenetic pathway. *Cell* **65,** 1203–1212 (1991).
26. Roemer, T., Madden, K., Chang, J. & Snyder, M. Selection of axial growth sites in yeast requires Axl2p, a novel plasma membrane glycoprotein. *Genes Dev.* **10,** 777–793 (1996).
27. Caviness, V. S. J., Takahashi, T. & Nowakowski, R. S. Numbers, time and neocortical neurogenesis: A general developmental and evolutionary model. *Trends Neurosci.* **18,** 379–383 (1995).
28. Chenn, A. & McConnell, S. K. Cleavage orientation and the asymmetric inheritance of Notch1 immunoreactivity in mammalian neurogenesis. *Cell* **82,** 631–641 (1995).
29. Bilder, D., Li, M. & Perrimon, N. Cooperative regulation of cell polarity and growth by *Drosophila* tumor suppressors. *Science* **289,** 113–116 (2000).
30. Lu, B., Ackerman, L., Jan, L. Y. & Jan, Y. N. Modes of protein movement that lead to the asymmetric localization of Partner of Numb during neuroblast division in *Drosophila*. *Mol. Cell* **4,** 883–891 (1999).

Acknowledgements

We thank J. Chant for helpful suggestions; S. Guo and Y.-M. Chan for critically reading the manuscript and members of the Jan lab for stimulating discussions; A. Wodarz, A. Brand and D. St Johnston for providing fly strains; A. Wodarz, T. Uemura and B. Chia for antibodies; M. Bienz for antibodies and GST–E-APC constructs. This work was supported by a NIMH grant to the Silvo Conte Center for Neuroscience Research at UCSF, a National Research Service Award from NIH (B.L.) and a HSFP Fellowship (F.R.). Y.N.J. and LY.J. are Investigators of the Howard Hughes Medical Institute.

Correspondence and requests for materials should be addressed to Y.N.J. (e-mail: ynjan@itsa.ucsf.edu).

Complexes of MADS-box proteins are sufficient to convert leaves into floral organs

Takashi Honma & Koji Goto*

Institute for Chemical Research, Kyoto University, Uji, 611-0011, Japan

Genetic studies, using floral homeotic mutants, have led to the ABC model of flower development. This model proposes that the combinatorial action of three sets of genes, the A, B and C function genes, specify the four floral organs (sepals, petals, stamens and carpels) in the concentric floral whorls[1,2]. However, attempts to convert vegetative organs into floral organs by altering the expression of *ABC* genes have been unsuccessful[3–5]. Here we show that the class B proteins of *Arabidopsis*, PISTILLATA (PI) and APETALA3 (AP3), interact with APETALA1

* Present address: Research Institute for Biological Sciences, Kayo-cho, Jobo, Okayama, 716-1241, Japan.

© 2001 Macmillan Magazines Ltd

(AP1, a class A protein) and SEPALLATA3 (SEP3, previously AGL9), and with AGAMOUS (AG, a class C protein) through SEP3. We also show that vegetative leaves of triply transgenic plants, 35S::PI;35S::AP3;35S::AP1 or 35S::PI;35S::AP3;35S::SEP3, are transformed into petaloid organs and that those of 35S::PI; 35S::AP3;35S::SEP3;35S::AG are transformed into staminoid organs. Our findings indicate that the formation of ternary and quaternary complexes of ABC proteins may be the molecular basis of the ABC model, and that the flower-specific expression of *SEP3* restricts the action of the *ABC* genes to the flower.

Most flowers consist of four types of floral organs in concentric whorls. The development of floral organs depends on the combinatorial action of genes, as proposed in the ABC model of flower development. This model proposes that the combinations of three classes of organ identity genes specify the four types of floral organs[1,2]. That is, class A genes specify sepals in the first whorl, a combination of class A and B genes specify petals in the second whorl, class B and C genes specify stamens in the third whorl, and class C genes specify carpels in the fourth whorl. In *Arabidopsis*, *APETALA1* (*AP1*) and *APETALA2* (*AP2*) are class A genes, *PISTILLATA* (*PI*) and *APETALA3* (*AP3*) are class B genes, and *AGAMOUS* (*AG*) is classified as a class C gene. Molecular cloning of these genes revealed that *AP1*, *PI*, *AP3* and *AG* encode members of the MADS family of transcription factors[6–10]. Plant MADS proteins consist of four domains (Fig. 1d): the MADS (M) domain, a highly conserved DNA-binding domain; the I domain, an intervening region; the K domain, which is involved in protein–protein interactions; and the C domain[11]. Homo- or heterodimers of MADS proteins recognize and bind the conserved DNA sequence, $CC(A/T)_6GG$, called the CArG box *in vitro*[12]. The ABC model, however, suggests that different combinations of MADS proteins activate different groups of target genes in each whorls. How homologous MADS transcription factors are modulated to obtain whorl-specific functions at the molecular level remains unknown. In addition, the ectopic expression of combinations of *ABC* genes does not result in the conversion of vegetative leaves into floral organs[3–5]. This suggests that other unknown factors are required for floral organ identity.

Interactions with a ternary factor, either an unrelated protein or another MADS protein, may be responsible for the modulation of DNA-binding specificity and transcriptional activity[13]. PI and AP3 form a heterodimer to bind the CArG box *in vitro*[7,12]. The *AP3* promoter has three CArG boxes, which are bound by the PI–AP3 complex, and *AP3* is autoregulated by *PI–AP3* (refs 4, 14–16). In transgenic plants that express *PI* and *AP3* constitutively (35S::PI;35S::AP3 plants), however, the *AP3* promoter and *GUS* fusion gene (*AP3::GUS*) is expressed only in the floral organs[4,16] (see Fig. 2a). When the transcriptional activation domain, VP16 (ref. 17), is fused with PI (35S::PI-VP16;35S::AP3), *AP3::GUS* is expressed throughout the plant (T.H. and K.G., unpublished data). These observations suggest that PI–AP3 requires a ternary factor that supplies a transcriptional activation domain and whose expression is flower-specific.

To identify the proposed ternary factor, we screened a flower complementary DNA library using the yeast two-hybrid system with both *PI* and *AP3* as a bait. We found 340 positive colonies from 5.9×10^7 clones. We have sequenced 170 of the positive clones, and identified 19 clones of *PI*, 18 of *SEP3*, 15 of *AP1* and 4 of *ATA20* out of the clones that appeared more than twice. *SEP3*, *AP1* or *ATA20* can interact only when both *PI* and *AP3* are expressed as a bait, and these interactions were confirmed by β-galactoside (β-gal) assay (Fig. 1a). *SEP3* (previously called *AGL9*) is a member of MADS-box genes and is expressed in whorls 2–4 (ref. 18). As ATA20 is an anther-specific, putatively secreted protein[19], we omitted *ATA20* from further analysis. No other cofactor-like genes bearing transcriptional-activator domains were identified. These results suggest that PI–AP3 complex primarily interacts with AP1 and SEP3. In other words, the interactions among MADS proteins may be the principal protein–protein interactions of floral MADS proteins. We

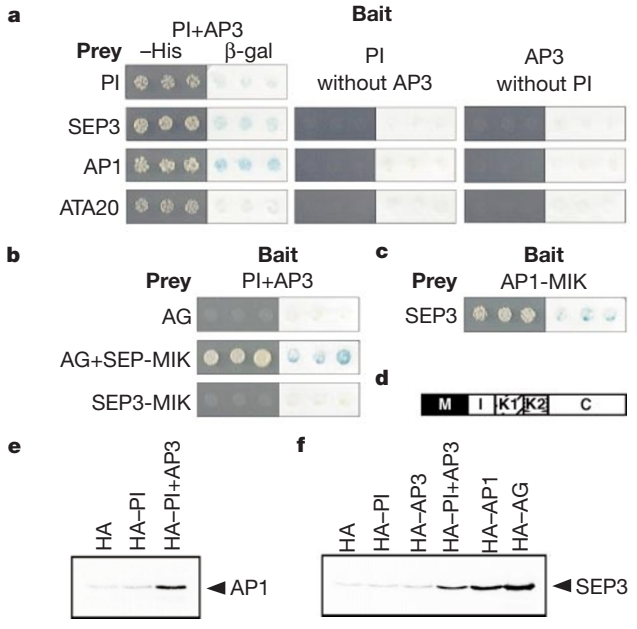

Figure 1 Interactions among MADS proteins in yeast and *in vitro*. **a**, Interactions between PI;LexA–AP3 and PI, SEP3, AP1 or ATA20 were confirmed by re-transformation on plates (–His) and a β-gal assay. No interaction occurred when either *PI* or *AP3* was removed from the bait vector. **b**, Interactions between PI–AP3 and AG are mediated by SEP3. MIK indicates the deletion of the C domain. **c**, Interactions between SEP3 and AP1-MIK. **d**, Diagram of plant MADS proteins. The K domain can be divided into two regions (K1, K2) on the basis of α-helix formation[22]. **e**, **f**, Co-immunoprecipitation of MADS proteins. Results are representative of four independent experiments.

Table 1 Transactivation assay of MADS proteins

(a) In yeast

MADS proteins	β-gal activity*		
	Full length	MIK†	K2C†
–‡	0.64 ± 0.03		
PI-VP16	148 ± 0.48		
PI	0.48 ± 0.02		
AP3	0.47 ± 0.01		
AP1	2.67 ± 0.14	0.49 ± 0.05	36.3 ± 0.45
SEP3	10.9 ± 0.63	0.46 ± 0.01	3.50 ± 0.17
AG	0.51 ± 0.01		

(b) In onion epidermal cells

Effectors	Relative LUC/R-LUC activity§
–¶	7.25 ± 0.88‖
35S::PI	6.00 ± 1.11
35S::PI-VP16	4.80 ± 1.01
35S::AP3	4.85 ± 0.76
35S::PI + 35S::AP3#	4.66 ± 0.70
35S::PI-VPI6 + 35S::AP3#	88.6 ± 12.8
35S::AP1	55.1 ± 6.09
35S::SEP3	142 ± 14.9
35S::AG	4.80 ± 1.09
35S::SEP1	63.1 ± 10.9
35S::SEP2	13.0 ± 2.86

*Mean ± s.e.m. × 10^{-1} Miller units. These data were calculated from five independent assays.
† Truncated protein deleting C domain (MIK) and MADS domain (K2C).
‡ GAL4-binding domain only (pAS2-1).
§ Transactivation activities were shown as arbitrary units of the LUC/R-LUC ratio from nine independent assays.
‖ Mean ± s.e.m. × 10^{-2}. These data were calculated from five independent assays.
¶ Vector with 35S promoter and nos terminator was used.
# Two plasmids were mixed.

© 2001 Macmillan Magazines Ltd

further examined interactions between PI–AP3 and AG. AG does not interact with PI–AP3 directly (Fig. 1b), but AG and SEP3 interact in yeast[20]. Yeast colonies survived only when all of *PI*, *AP3*, *AG* and *SEP3* were expressed (Fig. 1b). This result suggests that SEP3 mediates the interaction between PI–AP3 and AG.

We also examined the interactions between AP1 and SEP3, and found that these two proteins interact with each other (Fig. 1c). In these experiments, yeast, with full-length *AP1* or *SEP3* on the bait vector, survived without any prey. In contrast, when we used C-domain-deleted AP1 and SEP3 (*AP1-MIK* and *SEP3-MIK*), the yeast were not able to survive alone. This observation further suggests that AP1 and SEP3 have transcriptional activation domains[21]. The interactions of PI–AP3–AP1, PI–AP3–SEP3, AP1–SEP3 and AG–SEP3 were confirmed by immunoprecipitation experiments (Fig. 1e, f). As MADS proteins make a dimer to bind CArG boxes[22], and the formation of a tetramer enhances the binding affinity to CArG-box repeats[23], PI–AP3–AP1–SEP3 and PI–AP3–SEP3–AG are the most likely complexes in the second and the third whorls, respectively.

How do these quaternary complexes alter the activity of MADS transcription factors? We thought that AP1 or SEP3 might add transcriptional-activator domains to PI–AP3 and AG, which do not possess them, and therefore that either AP1 or SEP3 might contain transcriptional-activator domains. To test this hypothesis, we measured the transcriptional activity of MADS proteins in yeast and plant cells (Table 1). Whereas PI, AP3 and AG do not have any detectable activity, AP1 and SEP3 possess moderate and strong activities, respectively, in both yeast and plant cells. In yeast, the transcriptional activity of both AP1 and SEP3 is abolished by the deletion of the C domain and is retained in the K2-C domain, the region that is sufficient for interactions with PI–AP3 (T.H. and K.G., unpublished data). In onion epidermal cells, *PI* can activate the reporter gene (*CArG::LUC*) only when both the activation domain was fused to PI (*PI-VP16*) and *AP3* was co-introduced, and other results agree with yeast experiments. These results suggest that AP1 and SEP3 have transcriptional-activator domains, which are localized primarily within their C domains, and are able to supply them to PI–AP3 or AG following complex formation. As the C domain is the most divergent region among the plant MADS proteins[11], it is feasible that some MADS proteins have transcriptional activity and others do not.

Interactions among the MADS proteins may also modulate the DNA-binding affinity and, thus, their target genes. Examples of these interactions are found in the yeast MADS protein, MCM1, and in the *Antirrhinum* floral MADS proteins[13,23,24]. We carried out two *in vivo* assays to examine the modulating ability of the complexes of the *Arabidopsis* MADS proteins.

First, we crossed the *AP3::GUS* gene into 35S::PI, 35S::AP3, 35S::AP1 and 35S::SEP3 plants, and into plants with combinations of these transgenes. *AP3::GUS* expression was observed in various tissues of both 35S::PI;35S::AP3;35S::AP1 and 35S::PI;35S::AP3;35S::SEP3 triply transgenic plants, whereas *AP3::GUS* was expressed only in the floral organs of 35S::AP1, 35S::SEP3, 35S::PI, 35S::AP3 or 35S::PI;35S::AP3 plants (Fig. 2; and data not shown). These results suggest that ternary complexes, PI–AP3–AP1 and PI–AP3–SEP3, are sufficient to activate the *AP3* promoter. As both AP1 and SEP3 form homodimers (data not shown), dimers probably provide the activation domain and then tetramers increase the DNA-binding affinity[23], although monomers of AP1 and SEP3 are sufficient to supply the activation domain to PI–AP3.

Second, we examined the phenotype of the above triply transgenic plants and 35S::PI;35S::AP3;35S::SEP3;35S::AG quadruply transgenic plants. These plants show remarkable phenotypes: vegetative leaves were transformed into floral organs (Fig. 3). Sixty per cent (n = 55) of 35S::SEP3 transgenic lines show a severe dwarf phenotype, curled leaves, early flowering and terminal flowers (Fig. 3a), with the remainder displaying an intermediate phenotype. 35S::PI;35S::AP3 plants exhibit curled leaves (Fig. 3b) and flowers in which the outer two whorls are petals and the inner two whorls are stamens[4]. These transgenic plants fail to convert vegetative leaves into floral organs, but the first true leaves of 35S::PI;35S::AP3;35S::SEP3 plants (the parental 35S::SEP3 displayed a severe phenotype) were converted into petaloid organs (Fig. 3c; compare g with e and f). These results suggest that *PI–AP3–SEP3* is sufficient for the conversion of vegetative leaves into petaloid organs. As *ap1* mutants lack petals, *AP1* is essential for petal identity. When SEP3 is over-expressed, however, its homodimer increases and then replaces AP1–SEP3 function. The observation that cauline leaves of 35S::PI;35S::AP3;35S::AP1 were also converted into petaloid organs (Fig. 3d, h) suggests that AP1 homodimer can function as AP1–SEP3. The functional redundancy of AP1 and SEP3 may reflect the fact that these two proteins are relatively closely related as they belong to AP1–SEP superclade[25,26]. As 35S::SEP3 (severe);35S::AG plants are growth arrested and we were unable to obtain progeny, we used 35S::SEP3 (intermediate);35S::AG to construct 35S::PI;35S::AP3;35S::SEP3;35S::AG plants. Cauline leaves of this quadruply transgenic plant are converted into staminoid organs (Fig. 3i–o) and all floral organs are transformed into

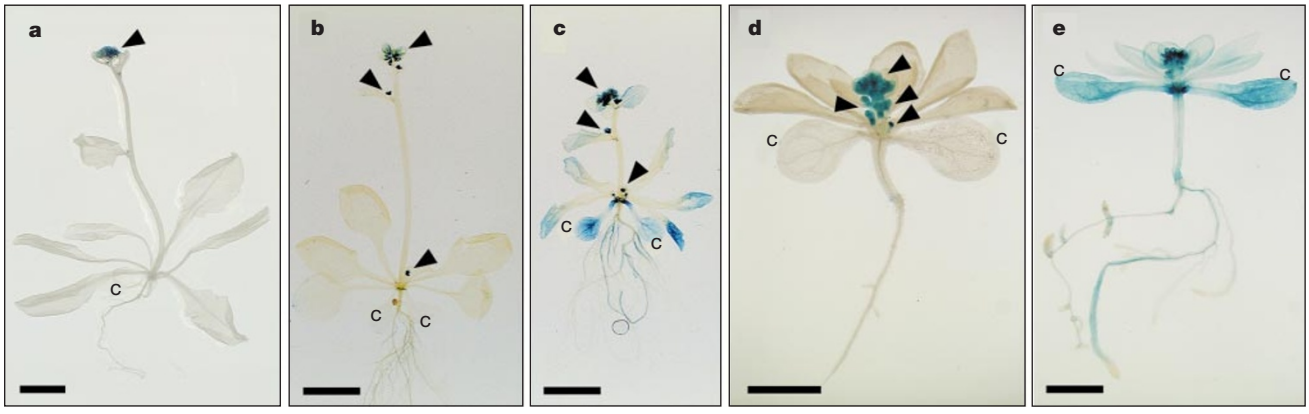

Figure 2 *AP3::GUS* expression in the transgenic plants. **a**, **b**, *AP3::GUS* in *35S::PI;35S::AP3* plants (**a**) and in *35S::AP1* plants (**b**). GUS activity was observed only in the flowers and floral buds (arrowheads). **c**, *AP3::GUS* in *35S::PI;35S::AP3;35S::AP1* triply transgenic plants. GUS activity was observed not only in floral organs (arrowheads), but also in roots, cotyledons, rosette and cauline leaves. **d**, *AP3::GUS* in a 3-week-old *35S::SEP3* plant. This line shows a severe phenotype. GUS expression is restricted to the floral organs (arrowheads). **e**, *AP3::GUS* in 17-day-old *35S::PI;35S::AP3;35S::SEP3* plants. GUS activity was observed in the whole plant. C; cotyledons. Scale bars, 5 mm (**a–c**); 1 mm (**d**, **e**).

© 2001 Macmillan Magazines Ltd

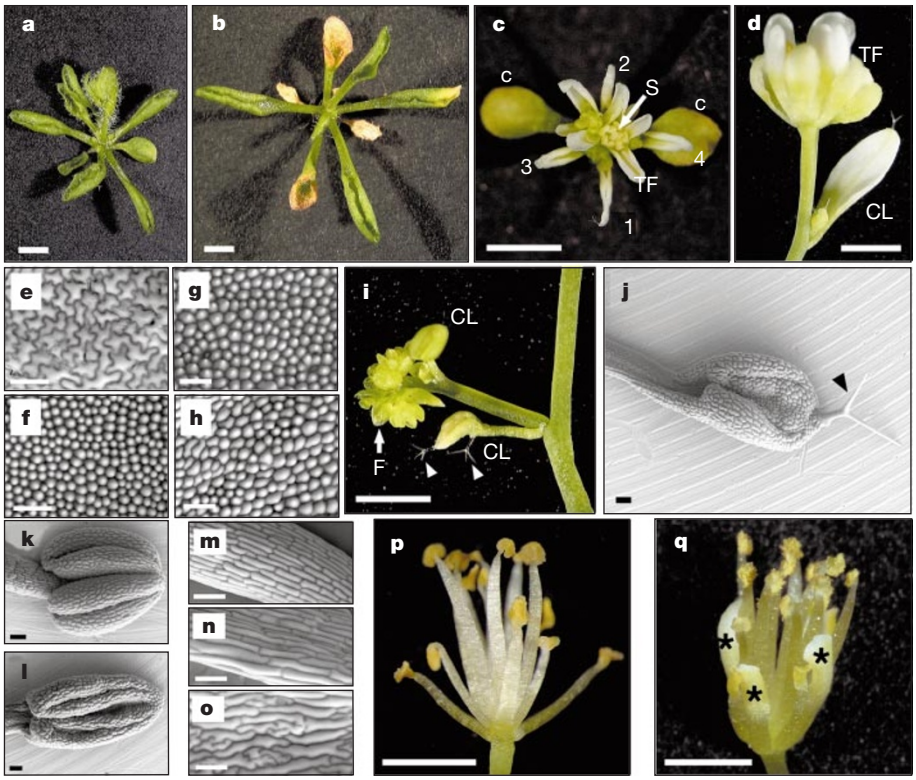

Figure 3 Phenotypes of triply and quadruply transgenic plants. **a**, Sixteen-day-old *35S::SEP3* plant showing a severe phenotype. **b**, Three-week-old *35S::PI;35S::AP3* plant displaying the curled leaf phenotype. **c**, Three-week-old *35S::PI;35S::AP3;35S::SEP3* plant. Cotyledons (C) are rather normal, but true leaves are transformed into petaloid organs. Numbers show the order of leaf development. S, stamens; TF, terminal flower. **d**, Three-week-old *35S::PI;35S::AP3;35S::AP1* plant. A cauline leaf (CL) is transformed into a petaloid organ. **e**–**h**, Cryo-scanning electron micrograph (cryo-SEM) of the adaxial surface of a *35S::SEP3* rosette leaf (**e**) which is similar to rosette and cauline leaves of the wild type; a wild-type petal (**f**); a petaloid *35S::PI;35S::AP3;35S::SEP3* rosette leaf (**g**); and a petaloid *35S::PI;35S::AP3;35::AP1* cauline leaf (**h**). The epidermis of vegetative leaves consists of irregular 'jigsaw-puzzle-shaped' cells with interspersed stomata (**e**), whereas petal epidermis consists of conical ridged cells and lacks stomata (**f**–**h**). **i**, Cauline leaves (CL) and lateral flowers (F) of *35S::PI;35S::AP3;35S::AG;35S::SEP3* quadruply transgenic plants. Not only all floral organs but also cauline leaves are transformed into stamens or staminoid organs. Arrowheads show branched trichomes. **j**–**o**, Cryo-SEM of staminoid cauline leaves of quadruply transgenic plants (**j**, **l**, **n**). For comparison, an anther (**k**), filament (**m**) and basal region of a cauline leaf (**o**) of wild-type are indicated. Wild-type cauline leaves lack a petiole and have irregularly shaped epidermal cells (**o**). Transformed cauline leaves of quadruply transgenic plants consist two distinct regions whose epidermal cells exhibit a morphology similar to that of wild-type anthers and filaments, respectively (**k**–**n**). **p**, **q**, Flowers of quadruply transgenic (**p**) and *35S::PI;35S::AP3;35S::AG* (**q**) plants. Asterisks show petaloid first whorl organs which are often incompletely converted into staminoid organs. Scale bars, 1 mm (**a**-**c**); 0.5 mm (**d**, **i**, **p**, **q**); 50 μm (**e**–**h**, **j**–**o**).

stamens or staminoid organs (Fig. 3p). 35S::PI;35S::AP3;35S::AG plants also have staminoid flowers, but first whorl organs, where SEP3 is not expressed, often remain incompletely transformed (Fig. 3q), and they never display the conversion from vegetative leaves into floral organs. These results suggest that *PI–AP3–AG–SEP3* activity is sufficient for the conversion of leaves into staminoid organs.

We have shown that SEP3 interacts with the PI–AP3 complex and also serves as a scaffold between PI–AP3 and AG. Ectopic expression of *PI–AP3–SEP3* and *PI–AP3–AP1* is sufficient to transform leaves into petaloid organs and that of *PI–AP3–SEP3–AG* is sufficient to convert cauline leaves into staminoid organs. These results indicate that floral organs can be formed independently of floral meristem, namely meristem identity and floral organ identity can be separated as suggested previously[27]. A target gene of PI–AP3 (*AP3::GUS*) is activated in non-floral organs when *SEP3* or *AP1* is expressed in addition to *PI–AP3*. Considering that SEP3 and AP1 can act as transcriptional activators, whereas PI, AP3 and AG are not able to do so, SEP3 and AP1 can provide transactivation domains to the ternary and quaternary complexes. A loss-of-function allele of *SEP3* has been detected by T-DNA insertion screening[5]. The *sep3* mutant shows a subtle phenotype, but in combination with both *sep1* and *sep2*, mutants of *AGL2* and *AGL4*, it shows a similar phenotype to *bc* double mutants[5]. In onion epidermal cells, SEP1 and SEP2 show moderate and weak transcriptional activity (Table 1), suggesting that these proteins can also supply activator domains to other MADS proteins. *SEP1* and *SEP2* genes are expressed in the floral whorls 1–4, and their redundant functions to *SEP3* suggest that SEP proteins confer completely functional activity on ABC proteins as transcription factors in the flower. 35S::SEP3, 35S::SEP1 and 35S::SEP2 plants do not show homeotic change of floral organs (T.H. and K.G., unpublished data), but 35S::SEP3 together with *B*, *C* genes can convert leaves into floral organs. These results suggest that *SEP* genes provide the flower-specific activity to the function of the *B*, *C* genes by making complexes of their gene products. We propose that the ABC model should be amended to include *SEP* genes, which provide flower-specific activity. It is interesting to note that this functional divergence was acquired during the evolution of homologous MADS genes. □

Methods

Yeast two-hybrid screening and the β-gal assay

For the screening assay, both *LexA–AP3* (*AP3* fused with the LexA DNA-binding domain) and *PI* were expressed by the bait vector, pBTM116 (ref. 28), so that *PI* would be cloned as a positive control. The bait and the cDNA library on pACT2 were transformed in yeast L40 (ref. 28) simultaneously. We screened at 22 °C, the optimum temperature for *Arabidopsis* growth because the initial screening at 30 °C yielded no positive colonies. Interactions in yeast were confirmed by re-transforming three independent colonies on plates without histidine but with 2 mM 3-aminotriazole (–His), and by a colony-lift β-gal assay. To

© 2001 Macmillan Magazines Ltd

examine the quaternary complex, *LexA–AP3* and *PI* were expressed on the bait vector, and *GAL4 AD-AG* and/or *SEP3-MIK* were expressed on the prey vector. When two genes were expressed on the same vector, they were both driven by ADH1 promoters. Amino-acid residues 1–167 and 1–171 were used for the truncated AP1-MIK and SEP3-MIK proteins, respectively. Other processes and the colony-lift β-gal assays were performed in accordance with the manufacturer's instructions (Clontech).

Immunoprecipitation

For immunoprecipitation experiments, radiolabelled AP1 or SEP3 were mixed with haemagglutinin (HA)-tagged proteins and precipitated with anti-HA antibody. Precipitated AP1 and SEP3 were separated by SDS–PAGE and detected by radio-imaging analyser, BAS2000 (Fujifilm). Other procedures were done as described[7,12].

Transactivation assay

For yeast, MADS proteins cDNAs were fused in-frame to GAL4 DNA-binding domain on pAS2-1 (Clontech) and transformed into the yeast strain YRG-2 (*UAS::lacZ*, Stratagene). AP1-K2C (residues 125–256) and SEP3-K2C (128–257) were used as truncated MADS proteins. Yeast cells were grown at 22 °C overnight, and the β-gal activity was assayed at 30 °C using *o*-nitrophenyl-β-D-galactopyranoside.

For onion epidermal cells, 35S promoter-driven MADS cDNAs that express native MADS proteins (effector) and *CArG::LUC* (reporter) were co-transfected into onion epidermal cells by using a particle delivery system (Bio-Rad). *CArG::LUC* has seven repeats of MADS protein binding consensus sequence[29], 5′-GGGGTGGCTTTCCTTTTTTGG TAAATTTTGGATCC-3′ (CArG box is underlined), upstream of the 35S minimal promoter (−30). 35S::*Renilla* luciferase (RLUC) was used for the internal control. LUC assays were conducted using Dual-luciferase reporter system (Promega). Other procedures were done as described[30].

Plant material

Arabidopsis Columbia ecotype was used for *Agrobacterium*-mediated vacuum transformation[31]. Plant crossing was carried out by manual cross-pollination. The presence of the transgenes was confirmed by PCR. *AP3::GUS* plants have a 600-base-pair region of the *AP3* promoter[16]. Staining for GUS activity was done as described[16].

Cryo-scanning electron micrograph

We used a Hitachi S-3500N scanning electron microscope equipped with a cryo-stage. For observation and photography, the stage was chilled at −20 °C and the natural scanning electron microscopy (SEM) mode (70 Pa) was used with a 25-kV accelerating voltage.

Received 2 October; accepted 6 November 2000.

1. Coen, E. S. & Meyerowitz, E. M. The war of the whorls: genetic interactions controlling flower development. *Nature* **353,** 31–37 (1991).
2. Bowman, J. L., Smyth, D. R. & Meyerowitz, E. M. Genetic interactions among floral homeotic genes of *Arabidopsis*. *Development* **112,** 1–20 (1991).
3. Mizukami, Y. & Ma, H. Ectopic expression of the floral homeotic gene AGAMOUS in transgenic *Arabidopsis* plants alters floral organ identity. *Cell* **71,** 119-131 (1992).
4. Krizek, B. A. & Meyerowitz, E. M. The *Arabidopsis* homeotic genes APETALA3 and PISTILLATA are sufficient to provide the B class organ identity function. *Development* **122,** 11–22 (1996).
5. Pelaz, S., Ditta, G. S., Baumann, E., Wisman, E. & Yanofsky, M. F. B and C floral organ identity functions require SEPALLATA MADS-box genes. *Nature* **405,** 200–203 (2000).
6. Mandel, M. A., Gustafson-Brown, C., Savidge, B. & Yanofsky, M. F. Molecular characterization of the *Arabidopsis* floral homeotic gene *APETALA1*. *Nature* **360,** 273–277 (1992).
7. Goto, K. & Meyerowitz, E. M. Function and regulation of the *Arabidopsis* floral homeotic gene PISTILLATA. *Genes Dev.* **8,** 1548–1560 (1994).
8. Jack, T., Brockman, L. L. & Meyerowitz, E. M. The homeotic gene *APETALA3* of *Arabidopsis thaliana* encodes a MADS box and is expressed in petals and stamens. *Cell* **68,** 683-697 (1992).
9. Yanofsky, M. F. *et al.* The protein encoded by the *Arabidopsis* homeotic gene *agamous* resembles transcription factors. *Nature* **346,** 35–39 (1990).
10. Schwarz-Sommer, Z., Huijser, P., Nacken, W., Saedler, H. & Sommer, H. Genetic control of flower development: homeotic genes in *Antirrhinum majus*. *Science* **250,** 931–936 (1990).
11. Ma, H., Yanofsky, M. F. & Meyerowitz, E. M. *AGL1-AGL6*, an *Arabidopsis* gene family with similarity to floral homeotic and transcription factor genes. *Genes Dev.* **5,** 484–495 (1991).
12. Riechmann, J. L., Krizek, B. A. & Meyerowitz, E. M. Dimerization specificity of *Arabidopsis* MADS domain homeotic proteins APETALA1, APETALA3, PISTILLATA, and AGAMOUS. *Proc. Natl Acad. Sci. USA* **93,** 4793–4798 (1996).
13. Herskowitz, I. A regulatory hierarchy for cell specialization in yeast. *Nature* **342,** 749–757 (1989).
14. Tilly, J. J., Allen, D. W. & Jack, T. The CArG boxes in the promoter of the *Arabidopsis* floral organ identity gene APETALA3 mediate diverse regulatory effects. *Development* **125,** 1647–1657 (1998).
15. Hill, T. A., Day, C. D., Zondlo, S. C., Thackeray, A. G. & Irish, V. F. Discrete spatial and temporal cis-acting elements regulate transcription of the *Arabidopsis* floral homeotic gene APETALA3. *Development* **125,** 1711–1721 (1998).
16. Honma, T. & Goto, K. The *Arabidopsis* floral homeotic gene PISTILLATA is regulated by discrete cis-elements responsive to induction and maintenance signals. *Development* **127,** 2021–2030 (2000).
17. Sadowski, I., Ma, J., Triezenberg, S. & Ptashne, M. GAL4-VP16 is an unusually potent transcriptional activator. *Nature* **335,** 563–564 (1988).
18. Mandel, M. A. & Yanofsky, M. F. The *Arabidopsis AGL9* MADS box gene is expressed in young flower primordia. *Sex Plant Reprod.* **11,** 22–28 (1998).
19. Rubinelli, P., Hu, Y. & Ma, H. Identification, sequence analysis and expression studies of novel anther-specific genes of *Arabidopsis thaliana*. *Plant Mol. Biol.* **37,** 607–619 (1998).
20. Fan, H. -Y., Hu, Y., Tudor, M. & Ma, H. Specific interactions between the K domains of AG and AGLs, members of the MADS domain family of DNA binding proteins. *Plant J.* **12,** 999–1010 (1997).
21. Cho, S. *et al.* Analysis of the C-terminal region of *Arabidopsis thaliana* APETALA1 as a transcription activation domain. *Plant Mol. Biol.* **40,** 419–429 (1999).
22. Riechmann, J. L. & Meyerowitz, E. M. MADS domain proteins in plant development. *J. Biol. Chem.* **378,** 1079–1101 (1997).
23. Egea-Cortines, M., Saedler, H. & Sommer, H. Ternary complex formation between the MADS-box proteins SQUAMOSA, DEFICIENS and GLOBOSA is involved in the control of floral architecture in *Antirrhinum majus*. *EMBO J.* **18,** 5370–5379 (1999).
24. Davies, B., Egea-Cortines, M., de Andrade Silva, E., Saedler, H. & Sommer, H. Multiple interactions amongst floral homeotic MADS box proteins. *EMBO J.* **15,** 4330-4343 (1996).
25. Rounsley, S. D., Ditta, G. S. & Yanofsky, M. F. Diverse roles for MADS box genes in *Arabidopsis* development. *Plant Cell* **7,** 1259–1269 (1995).
26. Smyth, D. A reverse trend—MADS functions revealed. *Trends Plant Sci.* **5,** 315–317 (2000).
27. Parcy, F., Nilsson, O., Busch, M. A., Lee, I. & Weigel, D. A genetic framework for floral patterning. *Nature* **395,** 561–566 (1998).
28. Bartel, P. L., Chien, C., Sternglanz, R. & Fields, S. in *Cellular Interactions in Development: a Practical Approach.* (ed. Hartley, D. A.) 153–179 (IRL Press, Oxford, 1993).
29. Shiraishi, H., Okada, K. & Shimura, Y. Nucleotide sequences recognized by the AGAMOUS MADS domain of *Arabidopsis thaliana* in vitro. *Plant J.* **4,** 385–398 (1993).
30. Pan, S., Sehnke, P. C., Ferl, R. J. & Gurley, W. B. Specific interactions with TBP and TFIIB in vitro suggest that 14-3-3 proteins may participate in the regulation of transcription when part of a DNA binding complex. *Plant Cell* **11,** 1591–1602 (1999).
31. Bechtold, N., Ellis, J. & Pelletier, G. *In planta Agrobacterium* mediated gene transfer by infiltration of adult *Arabidopsis* plants. *C. R. Acad. Sci. Paris* **316,** 1194–1199 (1993).

Acknowledgements

We are grateful to M. Yanofsky for communicating data before publication, and to D. Weigel for providing the cDNA library. We also thank J. Bowman, T. Ito and H. Tsukaya for critical reading of the manuscript. This work was supported by grants from the Monbusho and JSPS.

Correspondence and requests for materials should be addressed to K.G. (e-mail: kgoto@v004.vaio.ne.jp).

Genome sequence of enterohaemorrhagic *Escherichia coli* O157:H7

Nicole T. Perna*†, Guy Plunkett III‡, Valerie Burland‡, Bob Mau‡, Jeremy D. Glasner‡, Debra J. Rose‡, George F. Mayhew‡, Peter S. Evans‡, Jason Gregor‡, Heather A. Kirkpatrick‡, György Pósfai§, Jeremiah Hackett‡, Sara Klink‡, Adam Boutin‡, Ying Shao‡, Leslie Miller‡, Erik J. Grotbeck‡, N. Wayne Davis‡, Alex Lim‖, Eileen T. Dimalanta‖, Konstantinos D. Potamousis‡‖, Jennifer Apodaca‡‖, Thomas S. Anantharaman¶, Jieyi Lin#, Galex Yen*, David C. Schwartz*‡‖, Rodney A. Welch☆ & Frederick R. Blattner*‡

** Genome Center of Wisconsin, † Department of Animal Health and Biomedical Sciences, ‡ Laboratory of Genetics, ‖ Department of Chemistry, ¶ Department of Biostatistics, and ☆ Department of Medical Microbiology and Immunology, University of Wisconsin, Madison, Wisconsin 53706, USA*
§ Institute of Biochemistry, Biological Research Center, H-6701 Szeged, Hungary
 # Cereon Genomics, LLC, 45 Sidney Street, Cambridge, Massachusetts 02139, USA

The bacterium *Escherichia coli* O157:H7 is a worldwide threat to public health and has been implicated in many outbreaks of haemorrhagic colitis, some of which included fatalities caused by haemolytic uraemic syndrome[1,2]. Close to 75,000 cases of O157:H7 infection are now estimated to occur annually in the United States[3]. The severity of disease, the lack of effective treatment and the potential for large-scale outbreaks from contaminated food supplies have propelled intensive research on the pathogenesis and detection of *E. coli* O157:H7 (ref. 4). Here we have sequenced the genome of *E. coli* O157:H7 to identify candidate genes responsible for pathogenesis, to develop better methods of strain detection and to advance our understanding of

© 2001 Macmillan Magazines Ltd